EUROPEAN ORGANIZATION FOR NUCLEAR RESEARCH

CERN-PPE/95-182
12 December 1995

Measurement of η Production in Two and Three-Jet Events from Hadronic Z Decays at LEP

The L3 Collaboration

Abstract

The inclusive production of η mesons has been studied using 1.6 million hadronic Z decays collected with the L3 detector. The η multiplicity per event, the multiplicity for two-jet and three-jet events separately, and the multiplicity in each jet have been measured and compared with the predictions of different Monte Carlo programs. The momentum spectra of η in each jet have also been measured. We observe that the measured η momentum spectrum in quark-enriched jets agrees well with the Monte Carlo prediction while in gluon-enriched jets it is harder than that predicted by the Monte Carlo models.

Submitted to Phys. Lett. B

1 Introduction

The production of quarks and gluons from e^+e^- annihilation is well described by the Standard Model [1] while the subsequent non-perturbative hadron formation is still in an exploratory state, guided by phenomenological models. The two most widely used are the string and the cluster models, implemented respectively in the Monte Carlo programs JETSET 7.3 [2] and HERWIG 5.5 [3]. Both programs use the parton shower approach based on a leading-log perturbative QCD calculation to model fragmentation.

The η meson is well suited to study the hadronization, since a large fraction comes from fragmentation rather than decay. We analyzed the η production in the following contexts:

- the total η production rate per event; this production rate is predicted neither by QCD nor by fragmentation models and needs to be determined experimentally.
- the multiplicity of η mesons in quark and gluon jets; QCD predicts a general enhancement of the particle multiplicity in gluon jets with respect to quark jets at the same jet energy due to the higher color charge of the gluon, irrespective of the particle type. We call this effect the enhancement by QCD.
- the momentum spectrum of η mesons, both in quark and gluon jets; this spectrum is predicted by QCD inspired fragmentation models [2, 3]. An additional enhancement of isoscalar meson and glueball production, particularly at high momenta, in gluon jets with respect to quark jets has been predicted based on an independent fragmentation model [4]. We call this effect the enhancement from fragmentation.

The general enhancement of particle multiplicity in gluon jets is implemented in both of the Monte Carlo generators we use to compare to our data. Both approaches predict similar particle spectra; no enhancement of η production at high momenta in gluon jets is expected in either model.

We test the validity of the QCD enhancement by comparing the production rate of both π° and η in gluon jets relative to quark jets. Since the enhancement by QCD is implemented in the Monte Carlo programs used, this test is equivalent to comparing the rates per event in data and Monte Carlo separately for two-jet and three-jet events, after the total rate has been determined.

We investigate any additional enhancement of isoscalar mesons from fragmentation by focusing on deviations from Monte Carlo predictions in the production rate and spectrum for both π° and η found in gluon jets. Since the enhancement is not implemented in the Monte Carlo, it should appear as a deviation at high momentum only for η.

The η production rate in a gluon-enriched environment and the η momentum spectra have been previously measured [5–8]. Although indications of a potential enhancement from fragmentation were observed both in rate and spectrum, no firm conclusion was possible due to statistical limitations. In our own previous analysis [9] we observed a deviation of the measured η momentum spectrum from the Monte Carlo prediction. The increased number of hadronic Z decays recorded by L3 allows a further study of η production in quark-enriched and gluon-enriched jets.

2 The L3 Detector

The L3 detector is described in detail in Reference [10]. It consists of a central tracking chamber, a high resolution electromagnetic calorimeter composed of bismuth germanium oxide (BGO) crystals, a ring of plastic scintillation counters, a uranium calorimeter with proportional wire chamber readout, and a precise muon spectrometer. These detectors are installed in a 12 m diameter magnet which provides a uniform field of 0.5 T along the beam direction.

The central tracker consists of a time expansion chamber (TEC) with high spatial resolution in the plane normal to the beam, and a Z-chamber mounted just outside the TEC, supplementing the r/ϕ measurements with z measurement.

In this analysis only the barrel part ($42^\circ < \theta < 138^\circ$) of the electromagnetic calorimeter is used. The material preceding this detector amounts to less than 10% of a radiation length. In this region the energy resolution is 5% for photons and electrons of energy around 100 MeV, and is less than 2% for energies above 1 GeV. The angular resolution of electromagnetic clusters is better than 0.5° for energies above 1 GeV.

3 Event Selection

The selection of events of the type $e^+e^- \rightarrow$ hadrons is based on the energy measured in the electromagnetic and the hadron calorimeters. Events are accepted if they have high multiplicity and high and well balanced visible energy [11]. For the data taking period from 1991 to 1993, a total of 1.6 million events are selected as hadronic events.

We compare our data to 1.6 million events generated by JETSET and 0.4 million events generated by HERWIG. The events are passed through the L3 detector simulation program [12], which accounts for detector resolution, energy loss, multiple scattering, interactions and decays in the beam pipe and the detector. The events are processed by the same reconstruction, selection and analysis programs as the experimental data. We accept 99% of the simulated hadronic Z decays.

Jets are built from energy depositions (clusters) in the calorimeters using the LUCLUS jet finding algorithm [13]. LUCLUS is based on a jet resolution variable, d, measured in GeV. The two calorimetric clusters with the smallest d are combined if d does not exceed a chosen d_{join} value. For small opening angles, the variable d can be interpreted as the transverse momentum of one of the clusters with respect to the sum of the two cluster momenta. The procedure is repeated until all pairs of remaining clusters have d greater than d_{join}. The remaining clusters are then called jets if their energy exceeds 5 GeV. To remove background from high-energy leptons and photons we require more than 4 calorimetric clusters in a jet. Typically, a hadronic jet consists of 15 clusters. Jets are ordered according to their energies, jet 1 being the most energetic one.

We classify events with two jets as the two-jet events and events with three or more jets as the three-jet events. At $d_{join} = 5$ GeV, events with four or more jets are about 17% of the three-jet sample. Table 1 shows the measured three-jet event rate for different d_{join} values. We compare the measurement with the predictions from JETSET and HERWIG, before (Generator) and after (Detector) detector simulation. The measured rates are well described by the Monte Carlo predictions. In the following analysis we choose $d_{join} = 5$ GeV.

We use the JETSET Monte Carlo events to study the gluon-jet purity of the third jet. All except the two most energetic jets are included as the third jet. One approach is based on events generated using the parton shower (PS) model to describe the perturbative fragmentation

d_{join} (GeV)	Data	JETSET		HERWIG	
		Generator	Detector	Generator	Detector
3	64%	66%	65%	66%	63%
4	52%	54%	53%	54%	51%
5	43%	45%	43%	45%	42%
6	35%	38%	36%	38%	35%
7	29%	32%	29%	32%	29%

Table 1: The three-jet event rate for different d_{join} values compared with the JETSET and HERWIG Monte Carlo predictions, before (Generator) and after (Detector) detector simulation. The statistical uncertainty of the quoted numbers is negligible.

process. A jet is called quark jet if it is the closest jet in space to either one of the two primary quarks. The remaining jets are called gluon jets. In three-jet events 97% of jet 1 and 87% of jet 2 are associated with the two primary quarks, while the remaining jets correspond to gluon jets in 85% of the cases.

In a second approach we check the result with JETSET events where a second order matrix element calculation (ME) is used. For these events the primary gluon is well defined and allows the gluon jet to be determined. We find a gluon-jet purity for the third jet of 69%. The probabilities of jet 1 and 2 to originate from a quark are 90% and 78% respectively.

Both Monte Carlo approaches predict primary gluon enrichment for jet 3. The dependence of the gluon-jet purity on the jet resolution parameter is small for d_{join} values between 3 and 7 GeV.

η and π° mesons are reconstructed from their two-photon decays. The photon selection criteria are as follows:

- the electromagnetic cluster must be in the barrel region, $|\cos\theta| \leq 0.74$;
- the energy of the cluster must be greater than 500 MeV for η and 100 MeV for π°;
- the angle between the cluster and the nearest charged track must be greater than 50 mrad;
- the lateral shower shape of the cluster must be consistent with that of a photon.

We calculate the invariant mass, $M_{\gamma\gamma}$, of all two-photon combinations in the event. Since photons from π° decays contribute significantly to the combinatoric background of the η signal, we reject from the η sample all photons contained in a two-photon combination with an invariant mass consistent with the π° mass ($0.113 < M_{\gamma\gamma} < 0.157$ GeV).

A fit is made to the two-photon invariant mass spectrum in the η and π° mass regions using a Gaussian function to represent the signal and a third order polynomial to describe the background. Figure 1 shows the result of the fit in the η mass region for each jet. Jet 3 is usually broader and hence has a higher selection efficiency for photons. This is seen in Figure 1 where a better signal to noise ratio in the η mass spectrum is observed. The η or π° candidate is assigned to its closest jet in space.

The model parameters in the Monte Carlo programs JETSET and HERWIG have been adjusted to reproduce the global event properties [14] of hadronic Z decays. We therefore check if the Monte Carlo programs can also model the data in individual jets. Good agreement between data and Monte Carlo is found for the jet energy, the number of constituent energy clusters for the jets, electromagnetic cluster energy, shower shape parameters, as well as other quantities which affect the reconstruction of η and π°. As an example, Figure 2a shows the distribution of the χ^2 of the electromagnetic clusters in jet 3, which we obtain by comparing the energy deposition in the crystals of the cluster to that expected for a photon. For accepted photon candidates we require a χ^2 of less than 8. Figure 2b shows the distribution of the number of clusters in jet 3. Good agreement between the data and the Monte Carlo for both variables is observed. The same agreement is also seen for the variables of jets 1 and 2. The momentum spectrum of the η background (under the η peak within a mass window of 0.5< $M_{\gamma\gamma}$ <0.595 GeV) has been compared with the Monte Carlo prediction. Figure 3 shows that the ratio of data spectra to Monte Carlo spectra for each jet is flat. The same check has been done for π° and similar results are obtained. Therefore the Monte Carlo adequately describes the momentum spectrum of the background.

4 Multiplicity of η Production

For the two-jet and three-jet events, as well as for each jet type, we determine the number of η mesons from the Gaussian part of the fit to the invariant mass spectra, as shown in Figure 1. In the hadronic events we analyzed we find in total (15096 ± 233) η mesons.

We estimate the η reconstruction efficiency by applying the same procedure to JETSET Monte Carlo events. The efficiency value is used to correct the observed number of η mesons. The resulting η production multiplicity is shown in Table 2 for the different event types. The same procedure is used to determine the π° multiplicity, which is also shown in Table 2. The total η multiplicity with all event types is measured as:

$$0.93 \pm 0.01(\text{stat.}) \pm 0.09(\text{syst.}) - 0.06(\text{model}).$$

The value agrees well with our previous measurement [9].

Systematic errors are estimated by varying the photon selection cuts. An additional error comes from a small (4%) difference of the detector efficiency observed when measuring the η and π° multiplicities for the two detector hemispheres. The statistical uncertainty of the Monte Carlo is included in the systematic error.

We repeat the efficiency computation using HERWIG Monte Carlo events. The difference from the JETSET efficiency serves as an estimate for the model dependence of the result and is treated as an additional systematic error. It is shown separately in Tables 2, 3 and 4.

As already observed in previous analyses [9, 15], the overall η multiplicity (0.93) is not well reproduced by the Monte Carlo calculations (1.09 for JETSET [1)], 1.31 for HERWIG). This is true for both two-jet and three-jet events. In Table 2 we have therefore normalized the Monte Carlo η multiplicity in 2-jet events to the measurement, 0.75, as shown in Table 2. The scaling factors are 0.79 for the JETSET and 0.64 for the HERWIG Monte Carlos. It can be seen from the table that after the normalization, the predicted η multiplicities in three-jet events and all events are in agreement with the measurement. No scaling is necessary for π° multiplicities.

From the Table 2, we can form the following ratios of mean multiplicities:

$$\frac{<\eta \text{ in three-jet events}>}{<\eta \text{ in two-jet events}>} = 1.52 \pm 0.05(\text{stat.}) \pm 0.06(\text{sys.}) - 0.09(\text{model})$$

[1)] For the JETSET Monte Carlo the parameters PARJ(25) and PARJ(26) allow the overall η and η' production rate to be suppressed. We used PARJ(25) = 0.6 and PARJ(26) = 0.3 for the event generation. Changing PARJ(25) is equivalent to the normalization of the multiplicity.

Hadron	Event Type	Measured	Stat.	Syst.	Model diff.	JETSET	HERWIG
η	two-jet	0.75	± 0.02	± 0.07	-0.03	0.75	0.75
	three-jet	1.14	± 0.02	± 0.10	-0.11	1.02	0.97
	all	0.93	± 0.01	± 0.09	-0.06	0.87	0.84
π°	two-jet	8.61	± 0.03	± 0.29	-0.91	8.51	8.65
	three-jet	11.62	± 0.03	± 0.39	-2.01	11.32	11.42
	all	9.90	± 0.02	± 0.33	-1.39	9.72	9.81

Table 2: The measured η and π° production multiplicities for different event types, corrected for the η reconstruction efficiency calculated from JETSET Monte Carlo events. The statistical and systematic errors of the multiplicity measurements are given. The model difference indicates the difference obtained when using HERWIG instead of JETSET to estimate the η reconstruction efficiency. The Monte Carlo predictions are also given after being normalized to the measured η multiplicity in two-jet events, 0.75.

Hadron	Jet	Measured	Stat.	Syst.	Model diff.	JETSET	HERWIG
η	1	0.39	± 0.01	± 0.04	-0.01	0.39	0.39
	2	0.36	± 0.01	± 0.06	-0.03	0.36	0.36
π°	1	4.56	± 0.02	± 0.14	-0.47	4.43	4.51
	2	4.05	± 0.02	± 0.16	-0.44	4.08	4.14

Table 3: The η and π° production multiplicity for the jets of two-jet events compared with the JETSET and HERWIG Monte Carlo predictions. The Monte Carlo prediction for the η is scaled by 0.79 for JETSET and 0.64 for HERWIG.

Hadron	Jet	Measured	Stat.	Syst.	Model diff.	JETSET	HERWIG
η	1	0.39	± 0.02	± 0.07	$+0.01$	0.36	0.34
	2	0.32	± 0.01	± 0.03	-0.02	0.33	0.31
	3	0.41	± 0.01	± 0.03	-0.07	0.32	0.31
π°	1	4.11	± 0.02	± 0.16	-0.61	4.06	4.05
	2	3.77	± 0.02	± 0.14	-0.66	3.76	3.74
	3	3.67	± 0.02	± 0.12	-0.64	3.50	3.64

Table 4: The η and π° production multiplicity for the jets of three-jet events compared with the JETSET and HERWIG Monte Carlo predictions. The Monte Carlo prediction for the η is scaled by 0.79 for JETSET and 0.64 for HERWIG.

The corresponding number is 1.36 from JETSET and 1.29 from HERWIG.

$$\frac{<\pi^\circ \text{ in three-jet events}>}{<\pi^\circ \text{ in two-jet events}>} = 1.35 \pm 0.01(\text{stat.}) \pm 0.01(\text{syst.}) - 0.10(\text{model})$$

The corresponding number is 1.33 from JETSET and 1.32 from HERWIG.

This ratio is determined by the effect of general QCD enhancement combined with the average energy of each jet. It is independent of the particle type as seen from the Monte Carlo prediction. From the data we clearly see the general QCD enhancement. For η there is probably an additional enhancement.

To study this enhancement, the η production rate is measured for each of the jets in two and three-jet events. The systematic errors including the error from the Monte Carlo model are estimated as mentioned above. The resulting η and π° multiplicities in each jet are given in Table 3 and Table 4 for two and three-jet events. The measurements are compared with the predictions of JETSET and HERWIG, including the scaling factors mentioned above. The agreement is very good for all jets except for η in Jet 3 where the measured η production rate is somewhat higher than that predicted by Monte Carlo, while for π° no enhancement in Jet 3 is observed. This is consistent with the enhancement from fragmentation of isoscalars. In the following we perform a detailed analysis on the momentum spectra of η mesons in quark and gluon jets and compare them with those of π°.

5 The Momentum Spectrum of η

We measure the η momentum spectrum for each jet. The momentum, x_p, is expressed in units of the beam energy. For each x_p bin a fit is made to the two-photon invariant mass spectrum to determine the η production multiplicity. The results are expressed as an x_p-dependent production cross section, $1/\sigma_h \, d\sigma/dx_p$, where σ_h is the total hadronic cross section. The measured x_p-dependent η rates for two and three-jet events are summarized in Tables 5 and 6. Figure 4 shows the measurement compared with the JETSET prediction. The Monte Carlo predictions agree well with the measurements for two-jet events, as well as for the first two jets in three-jet events. In the third jet of three-jet events the measured spectrum is harder than the Monte Carlo prediction.

For comparison, Figure 5 shows the x_p distributions of π° for three-jet events compared with the JETSET predictions. The Monte Carlo adequately describes the π° momentum spectra for all three jets. This result is consistent with that from other LEP experiments [16].

Figure 6 shows the η momentum spectrum for quark-enriched jets (*i.e.* the two jets in two-jet events and the first two jets in three-jet events) and for gluon-enriched jets (*i.e.* jet 3) compared with the Monte Carlo predictions. To compare the data and Monte Carlo quantitatively, we define a $\chi^2 \equiv \sum_{i=1}^{\mathrm{N}} (\mu_i - \mu_i^{MC})^2/\sigma_i^2$, where μ_i is the measurement in bin i, μ_i^{MC} is the Monte Carlo prediction, σ_i is the quadratic sum of the statistical and systematic errors and N is the number of x_p bins. We treat the systematic errors as uncorrelated between the different x_p bins (which gives a conservative estimate of the χ^2). For the quark-enriched jets the measured spectrum agrees well with Monte Carlo predictions, with χ^2/ndf close to 1. However, for the gluon-enriched jet, the χ^2/ndf values are 55/5 for JETSET and 37/5 for HERWIG. These χ^2 values confirm the visible difference between the shape of the momentum spectrum in data and Monte Carlo for the gluon-enriched jet. As a further test we perform the same analysis for $d_{join} = 4$ and 6 GeV and get similar results.

	x_p range	Measurement	JETSET	HERWIG
Jet 1	$0.02 < x_p < 0.05$	$1.55 \pm 0.10 \pm 0.25$	1.85	1.75
	$0.05 < x_p < 0.08$	$1.16 \pm 0.07 \pm 0.12$	1.07	1.04
	$0.08 < x_p < 0.11$	$0.86 \pm 0.07 \pm 0.16$	0.75	0.78
	$0.11 < x_p < 0.15$	$0.59 \pm 0.06 \pm 0.13$	0.53	0.55
	$0.15 < x_p < 0.20$	$0.47 \pm 0.05 \pm 0.16$	0.34	0.36
	$0.20 < x_p < 0.30$	$0.33 \pm 0.05 \pm 0.12$	0.19	0.21
Jet 2	$0.02 < x_p < 0.05$	$1.59 \pm 0.10 \pm 0.24$	1.84	1.78
	$0.05 < x_p < 0.08$	$1.13 \pm 0.08 \pm 0.12$	1.07	1.03
	$0.08 < x_p < 0.11$	$0.70 \pm 0.06 \pm 0.11$	0.71	0.72
	$0.11 < x_p < 0.15$	$0.60 \pm 0.06 \pm 0.11$	0.46	0.49
	$0.15 < x_p < 0.20$	$0.44 \pm 0.05 \pm 0.10$	0.28	0.30
	$0.20 < x_p < 0.30$	$0.21 \pm 0.04 \pm 0.13$	0.13	0.16

Table 5: The measured momentum dependent η production rate for the jets of two-jet events. The first error is statistical and the second systematic. The predictions from JETSET and HERWIG are also given.

	x_p range	Measurement	JETSET	HERWIG
Jet 1	$0.02 < x_p < 0.05$	$1.23 \pm 0.11 \pm 0.24$	1.41	1.21
	$0.05 < x_p < 0.08$	$0.77 \pm 0.07 \pm 0.12$	0.85	0.76
	$0.08 < x_p < 0.11$	$0.57 \pm 0.06 \pm 0.15$	0.56	0.52
	$0.11 < x_p < 0.15$	$0.55 \pm 0.04 \pm 0.15$	0.37	0.36
	$0.15 < x_p < 0.20$	$0.23 \pm 0.03 \pm 0.06$	0.22	0.24
	$0.20 < x_p < 0.30$	$0.19 \pm 0.02 \pm 0.07$	0.11	0.12
Jet 2	$0.02 < x_p < 0.05$	$1.01 \pm 0.14 \pm 0.25$	1.51	1.26
	$0.05 < x_p < 0.08$	$0.78 \pm 0.07 \pm 0.20$	0.90	0.81
	$0.08 < x_p < 0.11$	$0.53 \pm 0.05 \pm 0.07$	0.54	0.52
	$0.11 < x_p < 0.15$	$0.35 \pm 0.03 \pm 0.06$	0.32	0.33
	$0.15 < x_p < 0.20$	$0.25 \pm 0.02 \pm 0.06$	0.17	0.18
	$0.20 < x_p < 0.30$	$0.09 \pm 0.01 \pm 0.03$	0.07	0.08
Jet 3	$0.02 < x_p < 0.05$	$1.85 \pm 0.11 \pm 0.27$	2.07	1.80
	$0.05 < x_p < 0.08$	$1.07 \pm 0.04 \pm 0.10$	0.85	0.86
	$0.08 < x_p < 0.11$	$0.50 \pm 0.02 \pm 0.04$	0.34	0.39
	$0.11 < x_p < 0.15$	$0.28 \pm 0.01 \pm 0.03$	0.14	0.16
	$0.15 < x_p < 0.20$	$0.10 \pm 0.01 \pm 0.01$	0.05	0.06
	$0.20 < x_p < 0.30$	$0.03 \pm 0.00 \pm 0.01$	0.01	0.01

Table 6: The measured momentum dependent η production rate for the jets of three-jet events. The first error is statistical and the second systematic. The predictions from JETSET and HERWIG are also given.

The observed harder η momentum spectrum for the gluon-enriched jet indicates that the fragmentation in gluon jets is the origin of the difference between the measured and predicted η momentum spectra in our previous paper [9]. Since the π° momentum spectra in quark and gluon jets are in good agreement with Monte Carlo predictions, the enhancement by QCD is correctly modelled. The fact that the η, which is an isoscalar, has a harder momentum spectrum in gluon jets than that predicted by Monte Carlo, is qualitatively consistent with the enhancement from fragmentation [4]. Other independent fragmentation models could also give a harder η momentum spectrum in gluon jets, see for example ref. [17].

6 Summary and Conclusion

The η multiplicity per event, measured using 1.6 million hadronic Z decays, is $0.93 \pm 0.01(\mathrm{stat.}) \pm 0.09(\mathrm{syst.}) - 0.06(\mathrm{model})$. We find that the π° production in three-jet events is enhanced with respect to that in two-jet events, as predicted by Monte Carlo with the general enhancement by QCD. For the η, the enhancement is stronger than both the π° enhancement and the Monte Carlo prediction. The measurement of the η multiplicity in each jet shows that this additional enhancement is from the gluon-enriched jet. The observed momentum spectrum of η mesons in gluon-enriched jets is also harder than predicted by the JETSET and HERWIG Monte Carlo programs. This difference is related to the modelling of the gluon fragmentation into isoscalars.

7 Acknowledgments

We would like to thank T. Sjöstrand for many valuable discussions. We wish to express our gratitude to the CERN accelerator divisions for the excellent performance of the LEP machine. We acknowledge the effort of all engineers and technicians who have participated in the construction and maintenance of this experiment.

The L3 Collaboration:

M.Acciarri,[27] A.Adam,[46] O.Adriani,[17] M.Aguilar-Benitez,[26] S.Ahlen,[11] B.Alpat,[34] J.Alcaraz,[26] J.Allaby,[18] A.Aloisio,[29] G.Alverson,[12] M.G.Alviggi,[29] G.Ambrosi,[34] H.Anderhub,[49] V.P.Andreev,[38] T.Angelescu,[13] D.Antreasyan,[9] A.Arefiev,[28] T.Azemoon,[3] T.Aziz,[10] P.Bagnaia,[37,18] L.Baksay,[44] R.C.Ball,[3] S.Banerjee,[10] K.Banicz,[46] R.Barillère,[18] L.Barone,[37] P.Bartalini,[34] A.Baschirotto,[27] M.Basile,[9] R.Battiston,[34] A.Bay,[23] F.Becattini,[17] U.Becker,[16] F.Behner,[49] Gy.L.Bencze,[14] J.Berdugo,[26] P.Berges,[16] B.Bertucci,[18] B.L.Betev,[49] M.Biasini,[18] A.Biland,[49] G.M.Bilei[34] J.J.Blaising,[18] G.J.Bobbink,[2] R.Bock,[1] A.Böhm,[1] B.Borgia,[37] A.Boucham,[4] D.Bourilkov,[49] M.Bourquin,[20] D.Boutigny,[4] E.Brambilla,[16] J.G.Branson,[40] V.Brigljevic,[49] I.C.Brock,[35] A.Buijs,[45] A.Bujak,[46] J.D.Burger,[16] W.J.Burger,[20] C.Burgos,[26] J.Busenitz,[44] A.Buytenhuijs,[31] X.D.Cai,[19] M.Campanelli,[49] M.Capell,[16] G.Cara Romeo,[9] M.Caria,[34] G.Carlino,[4] A.M.Cartacci,[17] J.Casaus,[26] G.Castellini,[17] R.Castello,[27] F.Cavallari,[37] N.Cavallo,[29] C.Cecchi,[20] M.Cerrada,[26] F.Cesaroni,[37] M.Chamizo,[26] A.Chan,[51] Y.H.Chang,[51] U.K.Chaturvedi,[19] M.Chemarin,[25] A.Chen,[51] C.Chen,[7] G.Chen,[7] G.M.Chen,[7] H.F.Chen,[21] H.S.Chen,[7] M.Chen,[16] X.Chereau,[4] G.Chiefari,[29] C.Y.Chien,[5] M.T.Choi,[43] L.Cifarelli,[39] F.Cindolo,[9] C.Civinini,[17] I.Clare,[16] R.Clare,[16] T.E.Coan,[24] H.O.Cohn,[32] G.Coignet,[4] A.P.Colijn,[2] N.Colino,[26] V.Commichau,[1] S.Costantini,[37] F.Cotorobai,[13] B.de la Cruz,[26] T.S.Dai,[16] R.D'Alessandro,[17] R.de Asmundis,[29] H.De Boeck,[31] A.Degré,[4] K.Deiters,[47] E.Dénes,[14] P.Denes,[36] F.DeNotaristefani,[37] D.DiBitonto,[44] M.Diemoz,[37] D.van Dierendonck,[2] F.Di Lodovico,[49] C.Dionisi,[37] M.Dittmar,[49] A.Dominguez,[40] A.Doria,[29] I.Dorne,[4] M.T.Dova,[19,♯] E.Drago,[29] D.Duchesneau,[4] P.Duinker,[2] I.Duran,[41] S.Dutta,[10] S.Easo,[34] Yu.Efremenko,[32] H.El Mamouni,[25] A.Engler,[35] F.J.Eppling,[16] F.C.Erné,[2] J.P.Ernenwein,[25] P.Extermann,[20] R.Fabbretti,[47] M.Fabre,[47] R.Faccini,[37] S.Falciano,[37] A.Favara,[17] J.Fay,[25] M.Felcini,[49] T.Ferguson,[35] D.Fernandez,[26] G.Fernandez,[26] F.Ferroni,[37] H.Fesefeldt,[1] E.Fiandrini,[34] J.H.Field,[20] F.Filthaut,[35] P.H.Fisher,[16] G.Forconi,[16] L.Fredj,[20] K.Freudenreich,[49] M.Gailloud,[23] Yu.Galaktionov,[28,16] S.N.Ganguli,[10] P.Garcia-Abia,[26] S.S.Gau,[12] S.Gentile,[37] J.Gerald,[5] N.Gheordanescu,[13] S.Giagu,[37] S.Goldfarb,[23] J.Goldstein,[11] Z.F.Gong,[21] E.Gonzalez,[26] A.Gougas,[5] D.Goujon,[20] G.Gratta,[33] M.W.Gruenewald,[8] V.K.Gupta,[36] A.Gurtu,[10] H.R.Gustafson,[3] L.J.Gutay,[46] B.Hartmann,[1] A.Hasan,[30] J.T.He,[7] T.Hebbeker,[8] A.Hervé,[18] K.Hilgers,[1] W.C.van Hoek,[31] H.Hofer,[49] H.Hoorani,[20] S.R.Hou,[51] G.Hu,[19] M.M.Ilyas,[19] V.Innocente,[18] H.Janssen,[4] B.N.Jin,[7] L.W.Jones,[3] P.de Jong,[16] I.Josa-Mutuberria,[26] A.Kasser,[23] R.A.Khan,[19] Yu.Kamyshkov,[32] P.Kapinos,[48] J.S.Kapustinsky,[24] Y.Karyotakis,[4] M.Kaur,[19,◇] M.N.Kienzle-Focacci,[20] D.Kim,[5] J.K.Kim,[43] S.C.Kim,[43] Y.G.Kim,[43] W.W.Kinnison,[24] A.Kirkby,[33] D.Kirkby,[33] J.Kirkby,[18] W.Kittel,[31] A.Klimentov,[16,28] A.C.König,[31] E.Koffeman,[2] O.Kornadt,[1] V.Koutsenko,[16,28] A.Koulbardis,[38] R.W.Kraemer,[35] T.Kramer,[16] W.Krenz,[1] H.Kuijten,[31] A.Kunin,[16,28] P.Ladron de Guevara,[26] G.Landi,[17] C.Lapoint,[16] K.Lassila-Perini,[49] P.Laurikainen,[22] M.Lebeau,[18] A.Lebedev,[16] P.Lebrun,[25] P.Lecomte,[49] P.Lecoq,[18] P.Le Coultre,[49] J.S.Lee,[43] K.Y.Lee,[43] C.Leggett,[3] J.M.Le Goff,[18] R.Leiste,[48] M.Lenti,[17] E.Leonardi,[37] P.Levtchenko,[38] C.Li,[21] E.Lieb,[48] W.T.Lin,[51] F.L.Linde,[2] B.Lindemann,[1] L.Lista,[29] Z.A.Liu,[7] W.Lohmann,[48] E.Longo,[37] W.Lu,[33] Y.S.Lu,[7] K.Lübelsmeyer,[1] C.Luci,[37] D.Luckey,[16] L.Ludovici,[37] L.Luminari,[37] W.Lustermann,[47] W.G.Ma,[21] A.Macchiolo,[17] M.Maity,[10] G.Majumder,[10] L.Malgeri,[37] A.Malinin,[28] C.Maña,[26] S.Mangla,[10] M.Maolinbay,[49] P.Marchesini,[49] A.Marin,[11] J.P.Martin,[25] F.Marzano,[37] G.G.G.Massaro,[2] K.Mazumdar,[10] D.McNally,[18] S.Mele,[29] L.Merola,[29] M.Meschini,[17] W.J.Metzger,[31] Y.Mi,[23] A.Mihul,[13] A.J.W.van Mil,[31] G.Mirabelli,[37] J.Mnich,[18] M.Möller,[1] B.Monteleoni,[17] R.Moore,[3] S.Morganti,[37] R.Mount,[33] S.Müller,[1] F.Muheim,[20] E.Nagy,[14] S.Nahn,[16] M.Napolitano,[29] F.Nessi-Tedaldi,[49] H.Newman,[33] A.Nippe,[1] H.Nowak,[48] G.Organtini,[37] R.Ostonen,[22] D.Pandoulas,[1] S.Paoletti,[37] P.Paolucci,[29] G.Pascale,[37] G.Passaleva,[17] S.Patricelli,[29] T.Paul,[34] M.Pauluzzi,[34] C.Paus,[1] F.Pauss,[49] Y.J.Pei,[1] S.Pensotti,[27] D.Perret-Gallix,[4] S.Petrak,[8] A.Pevsner,[5] D.Piccolo,[29] M.Pieri,[17] J.C.Pinto,[35] P.A.Piroué,[36] E.Pistolesi,[17] V.Plyaskin,[28] M.Pohl,[49] V.Pojidaev,[28,17] H.Postema,[16] N.Produit,[20] R.Raghavan,[10] G.Rahal-Callot,[49] P.G.Rancoita,[27] M.Rattaggi,[27] G.Raven,[40] P.Razis,[30] K.Read,[32] M.Redaelli,[27] D.Ren,[49] M.Rescigno,[37] S.Reucroft,[12] A.Ricker,[1] S.Riemann,[48] B.C.Riemers,[46] K.Riles,[3] O.Rind,[3] S.Ro,[43] A.Robohm,[49] J.Rodin,[16] F.J.Rodriguez,[26] B.P.Roe,[3] M.Röhner,[1] S.Röhner,[1] L.Romero,[26] S.Rosier-Lees,[4] Ph.Rosselet,[23] W.van Rossum,[45] S.Roth,[1] J.A.Rubio,[18] H.Rykaczewski,[49] J.Salicio,[18] J.M.Salicio,[26] E.Sanchez,[26] A.Santocchia,[34] M.E.Sarakinos,[22] S.Sarkar,[10] M.Sassowsky,[1] G.Sauvage,[4] C.Schäfer,[1] V.Schegelsky,[38] D.Schmitz,[1] P.Schmitz,[1] M.Schneegans,[4] B.Schoeneich,[48] N.Scholz,[49] H.Schopper,[50] D.J.Schotanus,[31] R.Schulte,[1] K.Schultze,[1] J.Schwenke,[1] G.Schwering,[1] C.Sciacca,[29] P.G.Seiler,[47] J.C.Sens,[51] L.Servoli,[34] S.Shevchenko,[33] N.Shivarov,[42] V.Shoutko,[28] J.Shukla,[24] E.Shumilov,[28] D.Son,[43] A.Sopczak,[48] V.Soulimov,[29] B.Smith,[16] T.Spickermann,[1] P.Spillantini,[17] M.Steuer,[16] D.P.Stickland,[36] F.Sticozzi,[16] H.Stone,[36] B.Stoyanov,[42] K.Strauch,[15] K.Sudhakar,[10] G.Sultanov,[19] L.Z.Sun,[21] G.F.Susinno,[20] H.Suter,[49] J.D.Swain,[19] X.W.Tang,[7] L.Tauscher,[6] L.Taylor,[12] Samuel C.C.Ting,[16] S.M.Ting,[16] O.Toker,[34] F.Tonisch,[48] M.Tonutti,[1] S.C.Tonwar,[10] J.Tóth,[14] A.Tsaregorodtsev,[38] G.Tsipolitis,[35] C.Tully,[36] H.Tuchscherer,[44] J.Ulbricht,[49] L.Urbán,[14] U.Uwer,[18] E.Valente,[37] R.T.Van de Walle,[31] I.Vetlitsky,[28] G.Viertel,[49] M.Vivargent,[4] R.Völkert,[48] H.Vogel,[35] H.Vogt,[48] I.Vorobiev,[28] A.A.Vorobyov,[38] An.A.Vorobyov,[38] L.Vuilleumier,[23] M.Wadhwa,[6] W.Wallraff,[1] J.C.Wang,[16] X.L.Wang,[21] Y.F.Wang,[16] Z.M.Wang,[21] A.Weber,[1] R.Weill,[23] C.Willmott,[26] F.Wittgenstein,[18] S.X.Wu,[19] S.Wynhoff,[1] J.Xu,[11] Z.Z.Xu,[21] B.Z.Yang,[21] C.G.Yang,[7] X.Y.Yao,[7] J.B.Ye,[21] S.C.Yeh,[51] J.M.You,[35] C.Zaccardelli,[33] An.Zalite,[38] P.Zemp,[49] J.Y.Zeng,[7] Y.Zeng,[1] Z.Zhang,[7] Z.P.Zhang,[21] B.Zhou,[11] G.J.Zhou,[7] J.F.Zhou,[1] Y.Zhou,[3] G.Y.Zhu,[7] R.Y.Zhu,[33] A.Zichichi,[9,18,19] B.C.C.van der Zwaan.[2]

1 I. Physikalisches Institut, RWTH, D-52056 Aachen, FRG[§]
III. Physikalisches Institut, RWTH, D-52056 Aachen, FRG[§]
2 National Institute for High Energy Physics, NIKHEF, and University of Amsterdam, NL-1009 DB Amsterdam, The Netherlands
3 University of Michigan, Ann Arbor, MI 48109, USA
4 Laboratoire d'Annecy-le-Vieux de Physique des Particules, LAPP,IN2P3-CNRS, BP 110, F-74941 Annecy-le-Vieux CEDEX, France
5 Johns Hopkins University, Baltimore, MD 21218, USA
6 Institute of Physics, University of Basel, CH-4056 Basel, Switzerland
7 Institute of High Energy Physics, IHEP, 100039 Beijing, China
8 Humboldt University, D-10099 Berlin, FRG[§]
9 INFN-Sezione di Bologna, I-40126 Bologna, Italy
10 Tata Institute of Fundamental Research, Bombay 400 005, India
11 Boston University, Boston, MA 02215, USA
12 Northeastern University, Boston, MA 02115, USA
13 Institute of Atomic Physics and University of Bucharest, R-76900 Bucharest, Romania
14 Central Research Institute for Physics of the Hungarian Academy of Sciences, H-1525 Budapest 114, Hungary[‡]
15 Harvard University, Cambridge, MA 02139, USA
16 Massachusetts Institute of Technology, Cambridge, MA 02139, USA
17 INFN Sezione di Firenze and University of Florence, I-50125 Florence, Italy
18 European Laboratory for Particle Physics, CERN, CH-1211 Geneva 23, Switzerland
19 World Laboratory, FBLJA Project, CH-1211 Geneva 23, Switzerland
20 University of Geneva, CH-1211 Geneva 4, Switzerland
21 Chinese University of Science and Technology, USTC, Hefei, Anhui 230 029, China
22 SEFT, Research Institute for High Energy Physics, P.O. Box 9, SF-00014 Helsinki, Finland
23 University of Lausanne, CH-1015 Lausanne, Switzerland
24 Los Alamos National Laboratory, Los Alamos, NM 87544, USA
25 Institut de Physique Nucléaire de Lyon, IN2P3-CNRS,Université Claude Bernard, F-69622 Villeurbanne Cedex, France
26 Centro de Investigaciones Energeticas, Medioambientales y Tecnologicas, CIEMAT, E-28040 Madrid, Spain[♭]
27 INFN-Sezione di Milano, I-20133 Milan, Italy
28 Institute of Theoretical and Experimental Physics, ITEP, Moscow, Russia
29 INFN-Sezione di Napoli and University of Naples, I-80125 Naples, Italy
30 Department of Natural Sciences, University of Cyprus, Nicosia, Cyprus
31 University of Nymegen and NIKHEF, NL-6525 ED Nymegen, The Netherlands
32 Oak Ridge National Laboratory, Oak Ridge, TN 37831, USA
33 California Institute of Technology, Pasadena, CA 91125, USA
34 INFN-Sezione di Perugia and Universitá Degli Studi di Perugia, I-06100 Perugia, Italy
35 Carnegie Mellon University, Pittsburgh, PA 15213, USA
36 Princeton University, Princeton, NJ 08544, USA
37 INFN-Sezione di Roma and University of Rome, "La Sapienza", I-00185 Rome, Italy
38 Nuclear Physics Institute, St. Petersburg, Russia
39 University and INFN, Salerno, I-84100 Salerno, Italy
40 University of California, San Diego, CA 92093, USA
41 Dept. de Fisica de Particulas Elementales, Univ. de Santiago, E-15706 Santiago de Compostela, Spain
42 Bulgarian Academy of Sciences, Central Laboratory of Mechatronics and Instrumentation, BU-1113 Sofia, Bulgaria
43 Center for High Energy Physics, Korea Advanced Inst. of Sciences and Technology, 305-701 Taejon, Republic of Korea
44 University of Alabama, Tuscaloosa, AL 35486, USA
45 Utrecht University and NIKHEF, NL-3584 CB Utrecht, The Netherlands
46 Purdue University, West Lafayette, IN 47907, USA
47 Paul Scherrer Institut, PSI, CH-5232 Villigen, Switzerland
48 DESY-Institut für Hochenergiephysik, D-15738 Zeuthen, FRG
49 Eidgenössische Technische Hochschule, ETH Zürich, CH-8093 Zürich, Switzerland
50 University of Hamburg, D-22761 Hamburg, FRG
51 High Energy Physics Group, Taiwan, China
§ Supported by the German Bundesministerium für Bildung, Wissenschaft, Forschung und Technologie
‡ Supported by the Hungarian OTKA fund under contract numbers 2970 and T14459.
♭ Supported also by the Comisión Interministerial de Ciencia y Technologia

$\sharp$ Also supported by CONICET and Universidad Nacional de La Plata, CC 67, 1900 La Plata, Argentina
$\diamondsuit$ Also supported by Panjab University, Chandigarh-160014, India

References

[1] S.L. Glashow, Nucl. Phys. **22** (1961) 579;
S. Weinberg, Phys. Rev. Lett. **19** (1967) 1264;
A. Salam, "Elementary Particle Theory", Ed. N. Svartholm, Stockholm, "Almquist and Wiksell", (1968), 367;
M. Gell-Mann, AcPA, Suppl. **IX** (1972) 733;
H. Fritzsch and M. Gell-Mann, 16th International Conference on High Energy Physics, Batavia, 1972; editors J.D. Jackson and A. Roberts, National Accelerator Laboratory (1972);
H. Fritzsch, M. Gell-Mann and H. Leutwyler, Phys. Lett. **B 47** (1973) 365;
D.J. Gross and F. Wilczek, Phys. Rev. Lett. **30** (1973) 1343;
D.J. Gross and F. Wilczek, Phys. Rev. **D 8** (1973) 3633;
H.D. Politzer, Phys. Rev. Lett. **30** (1973) 1346;
G. 't Hooft, Nucl. Phys. **B 33** (1971) 173.

[2] JETSET Monte Carlo Program:
T. Sjöstrand, Comp. Phys. Comm. **39** (1986) 347;
T. Sjöstrand and M. Bengtsson, Comp. Phys. Comm. **43** (1987) 367.

[3] HERWIG Monte Carlo Program:
G. Marchesini and B. Webber, Nucl. Phys. **B 310** (1988) 461;
I.G. Knowles, Nucl. Phys. **B 310** (1988) 571;
G. Marchesini *et al.*, Comp. Phys. Comm. **67** (1992) 465.

[4] C.Peterson and T.F.Walsh, Phys. Lett. **B 91** (1980) 455.

[5] JADE Collab., W.Bartel *et al.*, Phys. Lett. **B 130** (1983) 470;
JADE Collab., W.Bartel *et al.*, Z. Phys. **C 28** (1985) 343.

[6] ARGUS Collab., H.Albrecht *et al.*, Z. Phys. **C 46** (1990) 15.

[7] CRYSTAL BALL Collab., Ch.Bieler *et al.*, Z. Phys. **C49** (1991) 225.

[8] L3 Collab., O.Adriani *et al.*, Phys. Lett. **B286** (1992) 503.

[9] L3 Collab., O.Adriani *et al.*, Phys. Lett. **B 328** (1994) 223.

[10] L3 Collaboration, B. Adeva *et al.*, Nucl. Instr. and Meth. **A 289** (1990) 35;
L3 Collaboration, O. Adriani *et al.*, Phys. Rep. **236** (1993) 1.

[11] L3 Collaboration, M. Acciarri *et al.*, Z. Phys. **C 62** (1994) 551.

[12] The L3 detector simulation is based on GEANT Version 3.14, November 1990;
see R. Brun *et al.*, "GEANT 3", CERN DD/EE/84-1 (Revised), Sept. 1987.
The GHEISHA program (H. Fesefeldt, RWTH Aachen Report PITHA 85/02 (1985)) is used to simulate hadronic interactions.

[13] T. Sjöstrand, Comp. Phys. Comm. **28** (1983) 229.

[14] L3 Collab., B. Adeva *et al.*, Z. Phys. **C 55** (1992) 39;
W.G. Ma, Y.F. Wang, *"JETSET with Resonance Production"*, L3 internal Note 1516 (1993).
The parameters of HERWIG have been retuned using the data of heavy flavor decays. The parameters used are: CLMAX=3.2, QCDLAM=0.17, VPCUT=0.5, CLPOW=1.45, B1LIM=0.35.

[15] ALEPH Collab., D.Buskulic et al., Phys. Lett. **B 292** (1992) 210.

[16] DELPHI Collab., W. Adam et al., CERN-PPE/95-144, submitted to Z. Phys. **C**.

[17] I. Montvay, Phys. Lett. **B 84** (1979) 331.

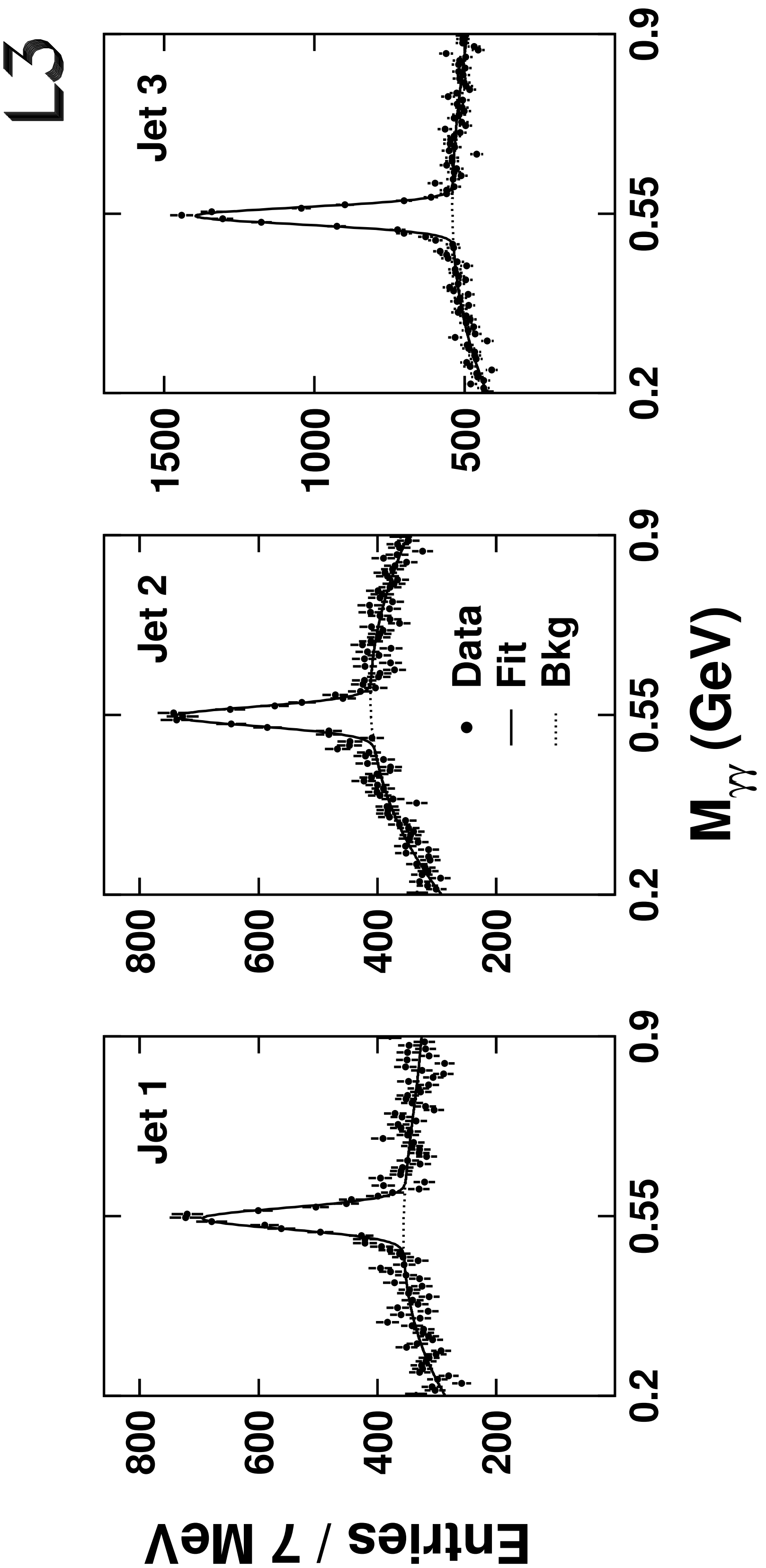

Figure 1: The $\gamma\gamma$ invariant mass spectrum for each jet in three-jet events. The number of two photon combinations are shown. The fit to the background and η signal is indicated.

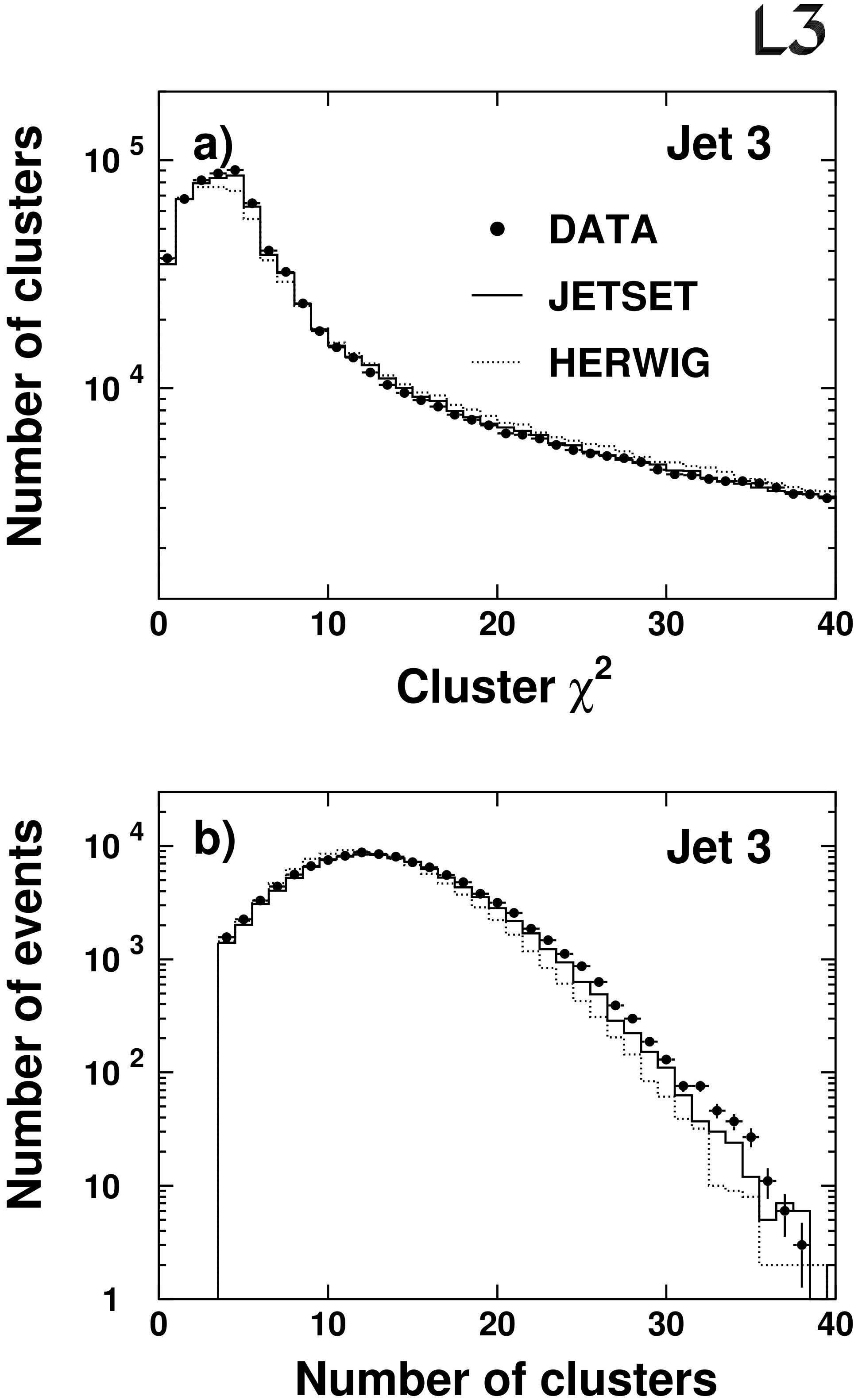

Figure 2: (a) The χ^2 distribution of the electromagnetic clusters and (b) the distribution of the number of clusters in the jet compared with the JETSET and HERWIG Monte Carlos. Both variables are shown for jet 3. The number of Monte Carlo events is normalized to the number of hadronic Z decays.

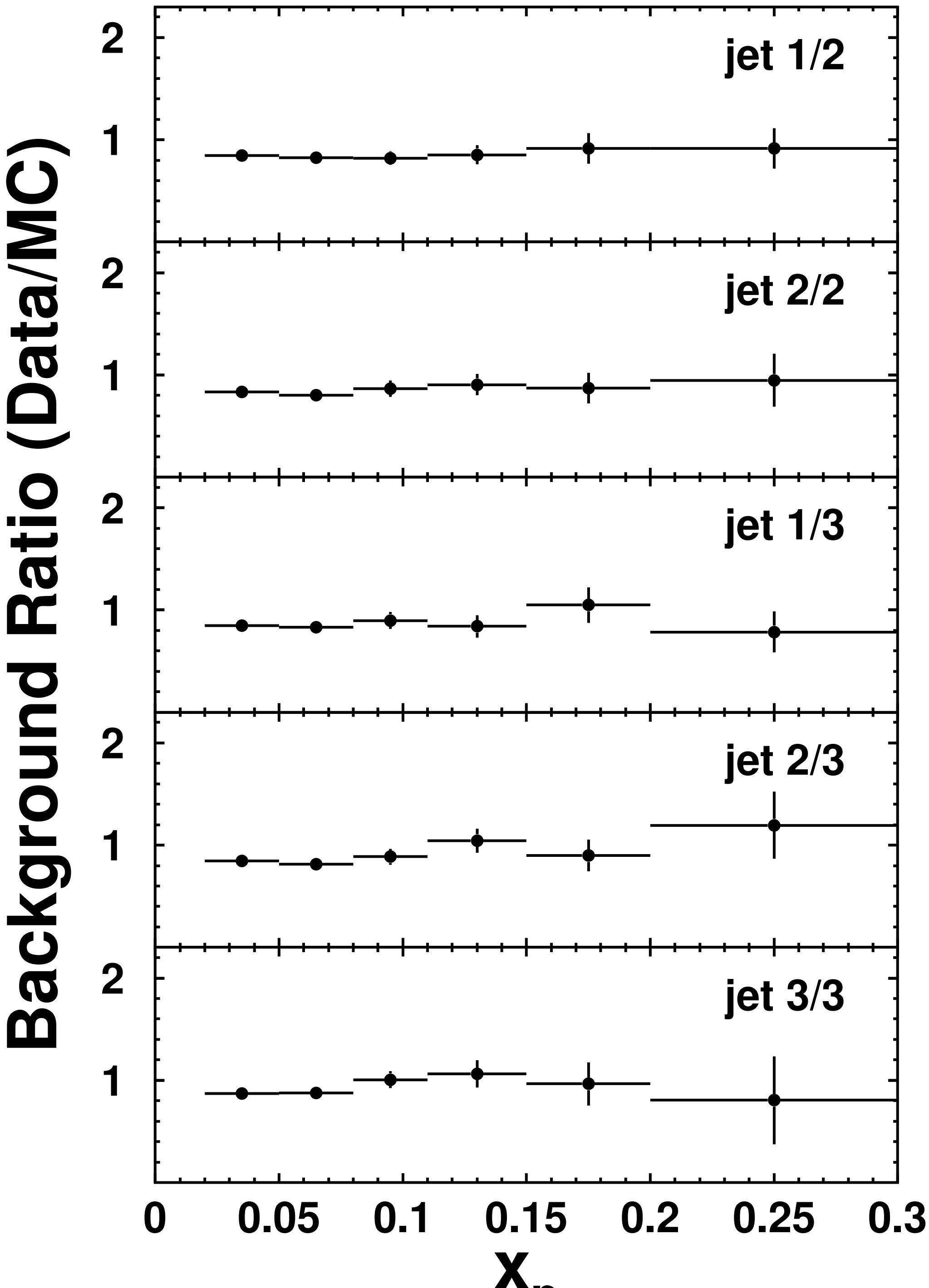

Figure 3: The ratio of the η background for each jet in the data and the Monte Carlo as a function of x_p. Jet 1/2 denotes the first jet in two-jet events, Jet 1/3 denotes the first jet in three-jet events, etc. x_p is defined as the momentum divided by the beam energy.

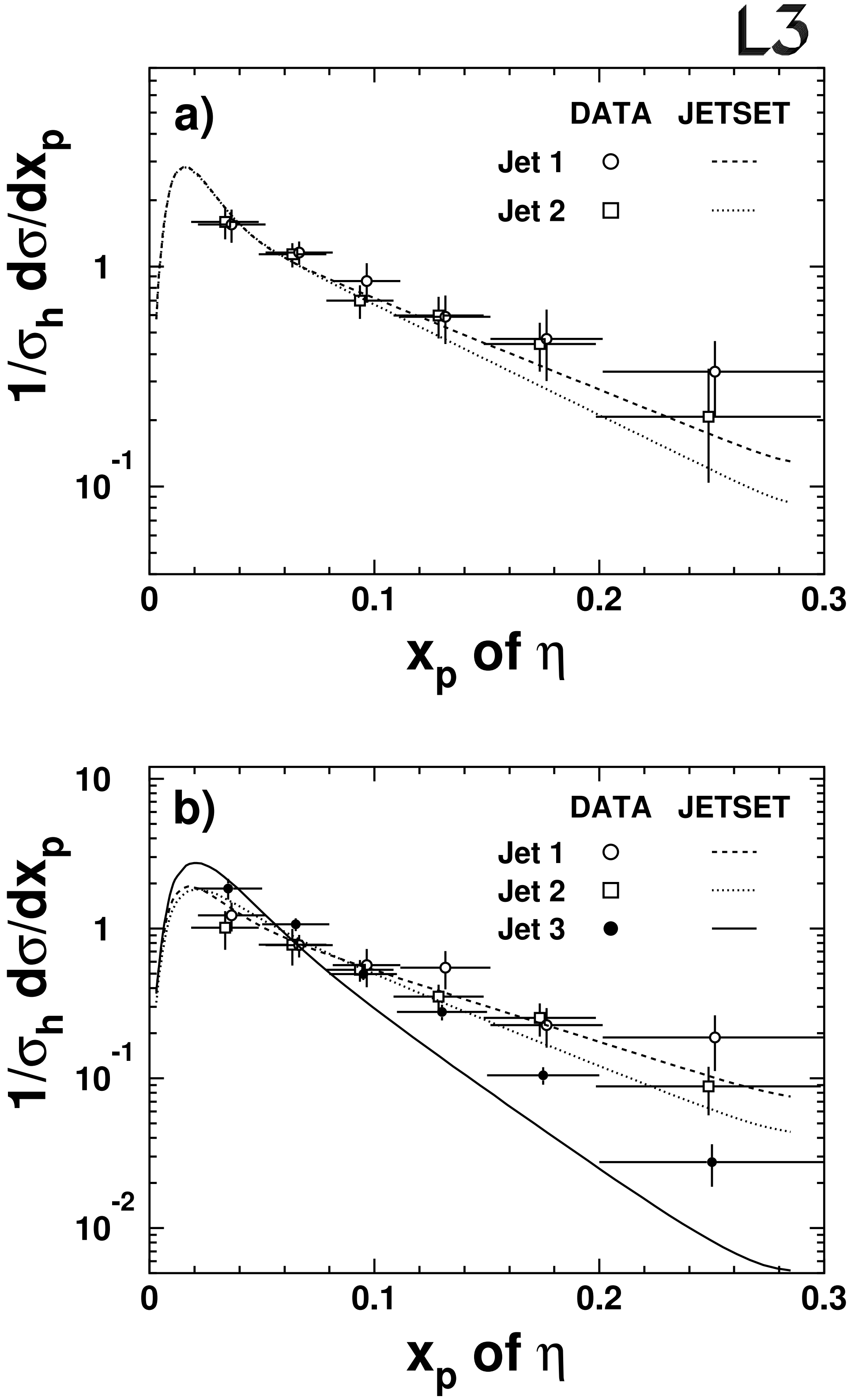

Figure 4: The measured x_p spectrum for inclusive η production (a) for two-jet and (b) for three-jet events compared with the JETSET predictions.

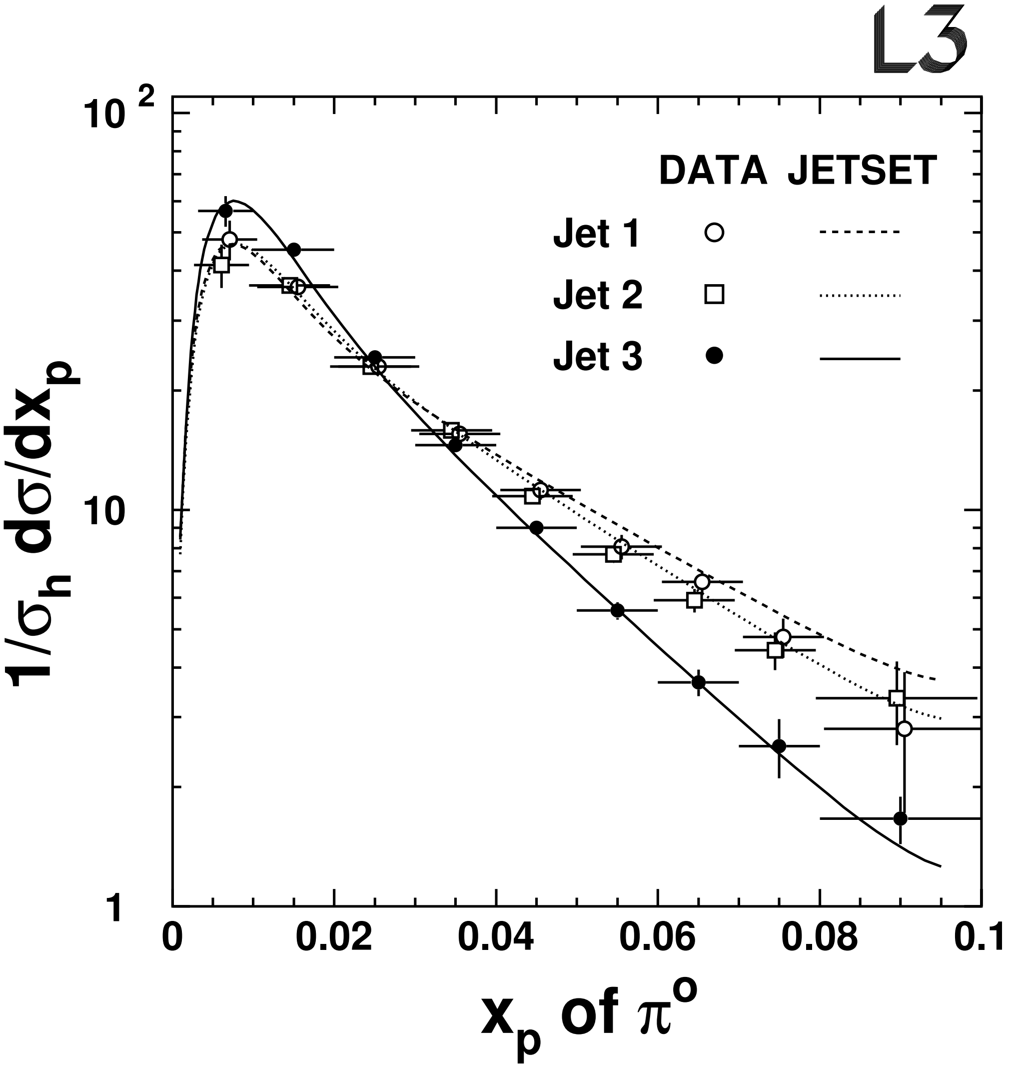

Figure 5: The measured x_p spectrum for inclusive π° production in each jet of three-jet events compared with the JETSET prediction.

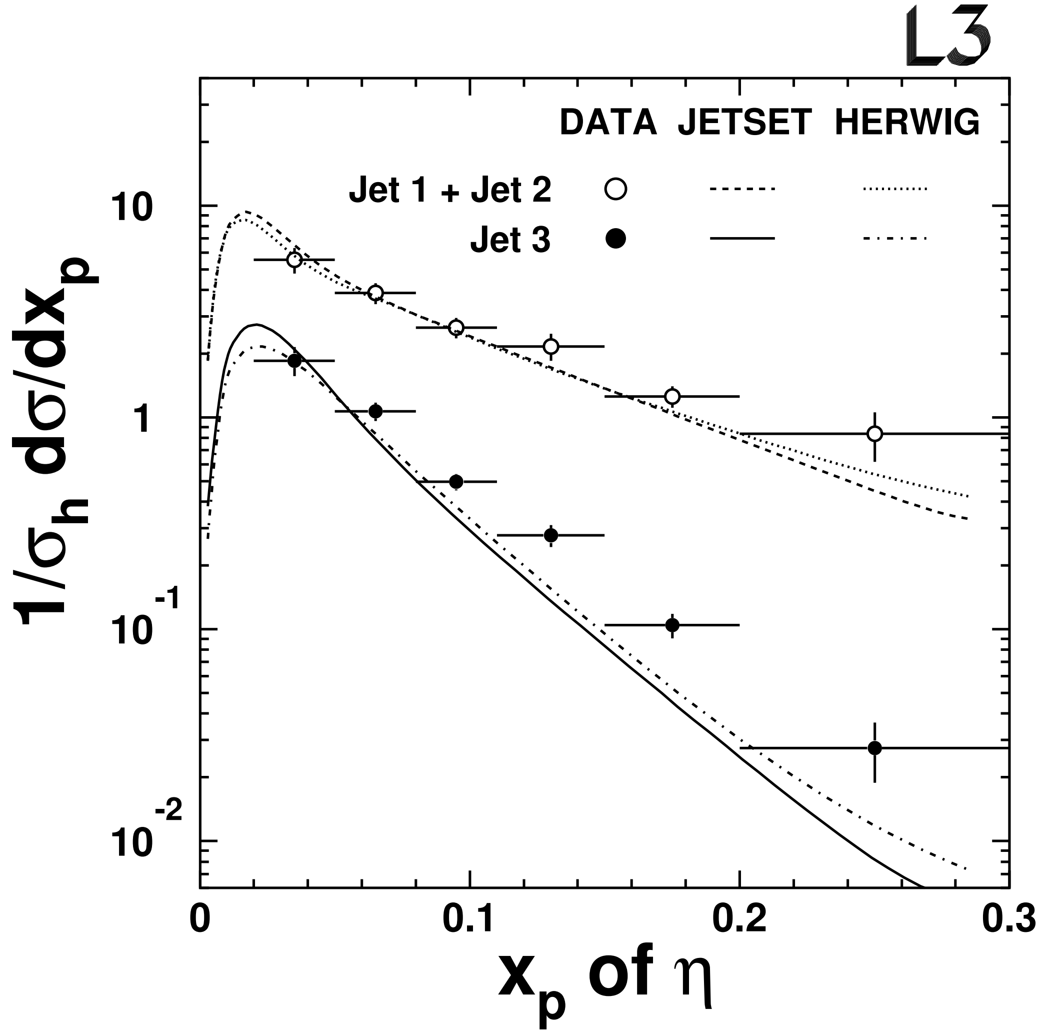

Figure 6: The measured x_p spectrum for inclusive η production for quark and gluon-enriched jets compared with the JETSET and HERWIG predictions.